Steady-State and Pre-Steady-State Kinetic Analysis of Halopropane Conversion by a *Rhodococcus* Haloalkane Dehalogenase[†]

Tjibbe Bosma, Mariël G. Pikkemaat, Jaap Kingma, John Dijk, and Dick B. Janssen*

Department of Biochemistry, Groningen Biomolecular Sciences and Biotechnology Institute, University of Groningen, Nijenborgh 4, 9747 AG Groningen, The Netherlands

Received September 26, 2002; Revised Manuscript Received December 15, 2002

ABSTRACT: Haloalkane dehalogenase from *Rhodococcus rhodochrous* NCIMB 13064 (DhaA) catalyzes the hydrolysis of carbon−halogen bonds in a wide range of haloalkanes. We examined the steady-state and pre-steady-state kinetics of halopropane conversion by DhaA to illuminate mechanistic details of the dehalogenation pathway. Steady-state kinetic analysis of DhaA with a range of halopropanes showed that bromopropanes had higher k_{cat} and lower K_M values than the chlorinated analogues. The kinetic mechanism of dehalogenation was further studied using rapid-quench-flow analysis of 1,3-dibromopropane conversion. This provided a direct measurement of the chemical steps in the reaction mechanism, i.e., cleavage of the carbon−halogen bond and hydrolysis of the covalent alkyl−enzyme intermediate. The results lead to a minimal mechanism consisting of four main steps. The occurrence of a pre-steady-state burst, both for bromide and 3-bromo-1-propanol, suggests that product release is rate-limiting under steady-state conditions. Combining pre-steady-state burst and single-turnover experiments indicated that the rate of carbon−bromine bond cleavage was indeed more than 100-fold higher than the steady-state k_{cat}. Product release occurred with a rate constant of 3.9 s^{-1}, a value close to the experimental k_{cat} of 2.7 s^{-1}. Comparing the kinetic mechanism of DhaA with that of the corresponding enzyme from *Xanthobacter autotrophicus* GJ10 (DhlA) shows that the overall mechanisms are similar. However, whereas in DhlA the rate of halide release represents the slowest step in the catalytic cycle, our results suggest that in DhaA the release of 3-bromo-1-propanol is the slowest step during 1,3-dibromopropane conversion.

Haloalkane dehalogenases comprise a group of enzymes that hydrolyze carbon−halogen bonds in a wide range of haloalkanes, some of which are notorious environmental pollutants. The potential use of haloalkane dehalogenases in bioremediation applications has stimulated intensive investigation of these enzymes (*1*), and there is a growing interest in the application of these enzymes as industrial biocatalysts (*2*). Three different haloalkane dehalogenases have been purified and characterized in detail: the enzymes from *Xanthobacter autotrophicus* GJ10 (DhlA)[1] (*3*), *Sphingomonas paucimobilis* UT26 (LinB) (*4*), and *Rhodococcus rhodochrous* NCIMB13064 (DhaA) (*5*). In addition, a number of haloalkane dehalogenases were previously isolated from Gram-positive haloalkane-utilizing bacterial strains m15-3 (*6*), HA1 (*7*), GJ70 (*8*), and Y2 (*9*). However, DNA sequencing showed that the corresponding haloalkane dehalogenase genes of these strains were identical to the *dhaA* gene of *R. rhodochrous* NCIMB13064 (*10*). The X-ray crystal structures of the haloalkane dehalogenases DhlA (*11*), LinB (*12*), and DhaA (*13*) are now available, and reveal that the enzymes belong to the α/β-hydrolase fold superfamily (*14*). Haloalkane dehalogenases have a globular structure and are composed of two domains: a large central catalytic domain with an α/β-hydrolase fold structure and a second domain which lies like a cap on the main domain. The latter domain emerges as a large α-helical excursion between β-strands 6 and 7 of the catalytic core. The interface of the two domains forms the hydrophobic active site. The catalytic triad residues are a nucleophilic aspartate, a base catalyst histidine, and an aspartate or glutamate as the third member. These amino acids form the basis of the dehalogenation reaction and are located in the main domain. Whereas there is significant sequence similarity in the catalytic core, the sequence and structure of the cap domain diverge considerably between different haloalkane dehalogenases. The cap domain was proposed to play a prominent role in determining substrate specificity (*15*).

Considerable understanding of the catalytic mechanism of haloalkane dehalogenases has emerged from studies with the enzyme from *X. autotrophicus* GJ10 (DhlA) (*16*−*20*). This enzyme contains a catalytic triad formed by Asp124, His289, and Asp260. The overall catalytic mechanism for dehalogenation occurs in four kinetically distinguishable steps. After formation of the Michaelis complex, the dehalogenation reaction proceeds via a nucleophilic attack of Asp124 on the halo-substituted carbon atom of the substrate, thereby displacing the halogen ion and forming an alkyl−enzyme intermediate. This covalent intermediate is subsequently

[†] This work was supported by a grant from Ciba Specialty Chemicals Inc. (Basel, Switzerland).

* To whom correspondence should be addressed. E-mail: D.B.Janssen@chem.rug.nl. Telephone: +31-50-3634209. Fax: +31-50-3634165.

[1] Abbreviations: DhaA, haloalkane dehalogenase from *R. rhodochrous*; DhlA, haloalkane dehalogenase from *X. autotrophicus* GJ10; LinB, haloalkane dehalogenase from *S. paucimobilis* UT2; SDS−PAGE, sodium dodecyl sulfate−polyacrylamide gel electrophoresis.

10.1021/bi026907m CCC: $25.00
Published on Web 06/13/2003

hydrolyzed by a water molecule activated by the dyad of His289 and Asp260. The resulting alcohol leaves the active site immediately, whereafter the halide ion is slowly released.

Haloalkane dehalogenase from *R. rhodochrous* NCIMB13064 (DhaA) is the first enzyme described to be involved in the degradation of several C_2-C_8 *n*-haloalkanes (*5*). The *dhaA* gene encodes a protein of 293 amino acids whose sequence is ~27% identical to that of DhlA. DhaA and DhlA have conserved amino acid residues involved in catalysis, suggesting that they have a similar reaction mechanism, yet they are adapted to different haloalkanes (*21*). Furthermore, DhaA has some structural features that might cause details of the dehalogenation mechanism to be different from those of DhlA. First, DhaA lacks a tryptophan residue equivalent to Trp175 of DhlA that is involved in substrate and halide binding. Both dehalogenases share a similar topology of two of the three residues comprising the catalytic triad, but the topological position of the carboxylate functionality of the triad is different. In DhaA, it is positioned at the end of β-strand 6, rather than after β-strand 7, as in DhlA and most other α/β-hydrolase fold enzymes (*13*, *22*).

DhlA and DhaA display different substrate specificities. DhaA is most active on longer chain (C_2-C_8), cyclic, and multiply halogenated alkanes. Recently, DhaA has drawn interest because of its capacity to slowly convert the environmentally and industrially important chlorinated hydrocarbon 1,2,3-trichloropropane (TCP). Mutants of DhaA with increased thermostability, and improved activity on TCP, have been obtained using directed evolution methods (*23*, *24*). DhlA uses preferably short chain haloalkanes (C_2-C_4) and exhibits the highest catalytic efficiency on 1,2-dibromoethane and 1,2-dichloroethane, whereas DhaA was not active on the latter compound (*20*, *25*, *26*). For DhlA, the rates of the separate steps involved in the dehalogenation pathway of its "natural substrate" 1,2-dichloroethane and the brominated analogue 1,2-dibromoethane have been established by applying a transient kinetic approach using a combination of rapid-quench-flow and stopped-flow fluorescence methodology. These studies showed that maximum turnover is controlled by a slow conformational change prior to halide release (*20*, *27*). For DhaA, such an analysis has not been carried out. However, to understand the selectivity of this dehalogenase on a mechanistic level, evaluation of the kinetic mechanism of DhaA is imperative. This paper describes such a kinetic characterization of DhaA. The steady-state kinetics were investigated with a range of mono-, di-, and trihalogenated propanes, which served as a basis for pre-steady-state analysis of 1,3-dibromopropane conversion. Since fluorescence quenching of DhaA is unsuitable for monitoring substrate and product binding, the kinetics of 1,3-dibromopropane conversion were studied using rapid-quench-flow techniques. The results of this work allow a comparison of the kinetic mechanism of DhaA and DhlA, and in this report, we highlight similarities and differences between these two haloalkane dehalogenases.

MATERIALS AND METHODS

Materials. All halogenated compounds that were used were obtained from commercial suppliers (Across, Merck, and Aldrich). ^2H_2O (99.8%, v/v) was purchased from Isotec Inc. (Miamisburg, OH).

Protein Expression and Purification. The haloalkane dehalogenase gene *dhaA* was amplified by PCR using total DNA of *Rhodococcus* sp. strain m15-3 as a template. The isolated *dhaA* gene was cloned into the T7-based expression vector pGEF$^+$, and overexpressed in *Escherichia coli* BL21-(DE3) (*10*). Because of the introduction of an *Nco*I restriction site for translational fusion into the ATG start codon, the second amino acid was changed from Ser to Ala.

The haloalkane dehalogenase was expressed and purified by DEAE-cellulose and hydroxylapatite chromatography according to the method of Schanstra et al. (*28*). Typically, 1.5 g of purified DhaA was isolated from a 5 L culture of *E. coli* BL21(DE3). The enzyme solution was concentrated with an Amicon ultrafiltration cell using a PM10 filter and stored at −20 or 4 °C in TEMAG [10 mM Tris-SO_4 (pH 7.5), 1 mM EDTA, 1 mM β-mercaptoethanol, 3 mM sodium azide, and 10% (v/v) glycerol]. The concentration of the purified DhaA was measured spectrophotometrically at 280 nm. An absorbance of 1 corresponds to 0.54 mg/mL, as calculated with DNAstar (DNASTAR, Inc., Madison, WI). The purity of the dehalogenase was analyzed by SDS−PAGE.

Steady-State Kinetics. Dehalogenase assays were carried out at 30 °C in 50 mM $NaHCO_3$/NaOH buffer (pH 9.4) using colorimetric detection of halide release from halogenated substrates (*3*). Solvent kinetic isotope effects were determined by performing dehalogenase assays in buffer containing halogenated substrate, and increasing concentrations of ^2H_2O. The K_m and V_{max} values were calculated from the initial rate of (halo)alcohol production, determined by gas chromatography, or from halide production rates, determined colorimetrically (*26*). The K_M value for 1,3-dibromopropane was determined by following substrate depletion by gas chromatography. A tube with a sufficient amount of enzyme and 50 μM 1,3-dibromopropane was incubated at 30 °C, and at different times within 20 min, samples of 1 mL were taken. The samples were extracted with 1.5 mL of diethyl ether containing 0.05 mM 1-bromohexane as the internal standard. The organic phase was analyzed by gas chromatography. Potassium bromide (80 mM), 3-bromo-1-propanol (20 mM), and 2-bromoethanol (20 mM) were tested as product inhibitors of 1,3-dibromopropane conversion by DhaA. Conversion of 1,3-dibromopropane was followed by gas chromatography.

Rapid-Quench-Flow Measurements. Single-turnover and pre-steady-state burst experiments on 1,3-dibromopropane conversion were carried out in 50 mM $NaHCO_3$/NaOH (pH 9.4) and 1 mM dithiothreitol at 30 °C using a Kintek RQF-3 rapid-quench-flow apparatus (KinTek Corp., State College, PA). The concentrations of enzyme and substrate cited in the text are those after mixing and during the enzymatic reaction. The reaction was initiated by rapidly mixing equal volumes (50 μL) of a concentrated enzyme solution and a freshly prepared 1,3-dibromopropane solution. At appropriate times, ranging from 2 ms to 0.5 s, the reaction was quenched with 120 μL of 0.8 M H_2SO_4. The quenched reaction mixture was directly extracted with 1.5 mL of ice-cold diethyl ether containing 0.05 mM 1-bromohexane as the internal standard, and then neutralized by the addition of $NaHCO_3$. The ether phase containing noncovalently bound substrate and halo alcohol was analyzed by gas chromatography, and the amount of bromide in the water phase was measured by ion chromatography.

Data Analysis. Numerical integration was performed by using Dynafit (*29*) (Biokin, Ltd., Madison, WI). The entire data set was fit to a single mechanism and a single set of rate constants. The 95% confidence interval for the rate constants was determined by a systematic search in the parameter space using an algorithm implemented in the program. An iterative process, varying one rate constant at a time, was used to fit the data. Initial estimates of k_2, k_3, and k_4 were obtained from the fits of the pre-steady-state burst data to the biphasic burst equation (*30*):

$$\text{product} = A \times \exp(-k_b t) + k_{ss} t$$

where A is the amplitude of the burst, k_b is the first-order rate constant of the pre-steady-state exponential phase, and k_{ss} is the rate of the linear phase which corresponds to the steady-state rate. The data were fit to the biphasic burst equation by nonlinear regression analysis using SigmaPlot (Jandell Scientific).

Analytical Methods. Concentrations of organic halogenated compounds were quantitatively determined by gas chromatography on a Chrompack 438S gas chromatograph equipped with a flame ionization detector and an HP wax column (length of 25 m, inner diameter of 0.2 mm, and film thickness of 0.2 μm) (Hewlett-Packard). Nitrogen was used as the carrier gas (50 kPa), and the temperature program was as follows: isothermal for 3 min at 45 °C followed by an increase to 220 °C at a rate of 10 °C/min.

Bromide concentrations in the water phase were quantitated by ion chromatography on a Dionex ion chromatograph with an AS12A column (length of 25 cm and diameter of 4 mm) and an AG12A precolumn (length of 4 cm and diameter of 4 mm). The carrier liquid was 270 mM Na_2CO_3 and 30 mM $NaHCO_3$.

RESULTS AND DISCUSSION

Steady-State Kinetics of Halopropane Conversion. The *dhaA* gene was heterologously expressed under control of the T7 promoter in *E. coli* BL21(DE3), and the dehalogenase was purified to homogeneity. The purified enzyme was used to determine the steady-state kinetic constants on a range of halopropanes, including the important environmental chemicals 1,2-dichloropropane and 1,2,3-trichloropropane. Both chloro- and bromopropanes are substrates for DhaA (Table 1). In agreement with previous results, bromopropanes are better substrates with turnover numbers (k_{cat}) that are higher than those of chlorinated analogues (*25*, *26*). In terms of catalytic efficiency (k_{cat}/K_M), 1,3-dibromopropane was the best substrate. Furthermore, DhaA converted different brominated propanes with a similar k_{cat} value. The higher affinity of DhaA for brominated compounds might be a consequence of tight substrate binding in combination with a high rate of carbon−bromine bond cleavage, as was observed for 1,2-dibromoethane conversion by DhlA, the corresponding enzyme from *X. autotrophicus* GJ10 (*20*). DhaA dehalogenated mono- and dibrominated propanes with a catalytic efficiency similar to that of DhlA, whereas the catalytic efficiency of DhaA on 1,2,3-tribromopropane was ~30-fold higher (*25*, *26*). This observation is consistent with the larger active site cavity of DhaA that can probably better accommodate large bulky substrates such as 1,2,3-tribromopropane (*13*). DhaA dehalogenated the different chlorinated propanes with considerable differences in maximum turnover as well as affinity. Within this series of substrates, DhaA has the highest efficiency toward 1,3-dichloropropane. Both 1,2-dichloropropane and 1,2,3-trichloropropane are poor substrates. DhaA slowly dehalogenated 1,2,3-trichloropropane with a low k_{cat} and high K_M, whereas no significant activity was detected for 1,2-dichloropropane. The opposite applies for DhlA, which is not active on 1,2,3-trichloropropane but slowly dehalogenated 1,2-dichloropropane (*20*, *26*).

Table 1: Steady-State Activity Parameters of Purified DhaA at pH 9.4 and 30 °C

substrate	k_{cat} (s^{-1})	K_m (mM)	k_{cat}/K_m (M^{-1} s^{-1})
1-chloropropane	0.48	1.0	480
1,2-dichloropropane	*a*		
1,3-dichloropropane	1.3	0.63	2000
1,2,3-trichloropropane	0.08	2.2	36
1-bromopropane	2.7	0.6	4500
1,2-dibromopropane	2.3	1.0	2300
1,3-dibromopropane	2.7	0.005	540000
1,2,3-tribromopropane	3.6	0.3	12000
1,2-dibromoethane	14.3	4.0	3600
3-bromo-1-propanol	3.0	3.3	910
2-bromoethanol[b]	>3.0	>11.0	>272

[a] Not detectable, detection limit of <10 milliunits/mg of protein at 10 mM substrate. [b] Due to the high background, only k_{cat}/K_M could be determined, setting lower limits for the k_{cat} and K_M values. The k_{cat} values had errors of less than 15%, and the K_m values had errors of less than 25%.

Compared to DhaA, the *Xanthobacter* dehalogenase has a more restricted substrate range. The latter dehalogenase exhibits the highest activity on smaller compounds such as its natural substrate 1,2-dichloroethane and the brominated analogue and nematocide 1,2-dibromoethane (*20*). Interestingly, DhaA converted 1,2-dibromoethane at a steady-state rate that is 4−5-fold higher than that found with DhlA, even though 1,2-dichloroethane is not a substrate for DhaA (*20*, *25*, *26*).

DhaA was also active on polar compounds such as 3-bromo-1-propanol and 2-bromoethanol, which are the products of enzymatic dehalogenation of 1,3-dibromopropane and 1,2-dibromoethane, respectively. Maximum turnover rates for these halo alcohols were similar to those found for the brominated propanes, whereas the K_M values were higher. Both halohydrins were examined as product inhibitors of 1,3-dibromopropane conversion. DhaA was inhibited by 3-bromo-1-propanol, whereas 2-bromoethanol did not inhibit 1,3-dibromopropane conversion. Since 3-bromo-1-propanol is a substrate for DhaA with a reasonably high affinity, this substrate is most likely a competitive inhibitor.

Bromide also inhibited DhaA. In the presence of 80 mM bromide, the maximum turnover rate on 1,3-dibromopropane dropped 10-fold. Since the K_M is too low to measure accurately, we were not able to determine a clear effect on the K_M in the presence of bromide. However, it seems likely that halide binds to both the free enzyme and the enzyme−substrate complex, since X-ray crystallography data for different haloalkane dehalogenases indicate that halides can bind in the active site region of these enzymes (*12*, *13*, *16*, *31*). This suggests that bromide exerts a noncompetitive type of inhibition, most likely mixed, on DhaA. Surprisingly, Schindler et al. (*25*), using an assay dependent on pH changes, did not find halide inhibition of DhaA at concentrations up to 80 mM.

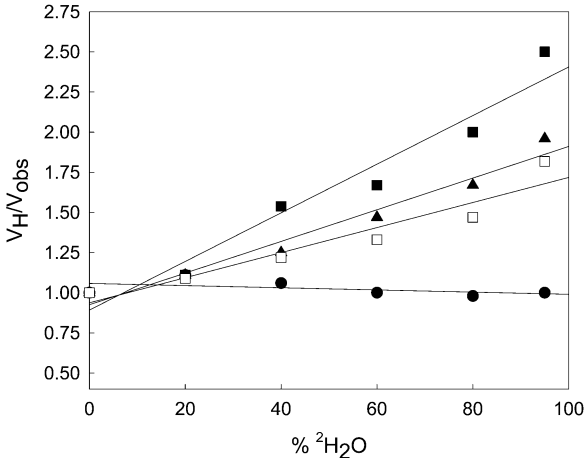

FIGURE 1: Solvent kinetic isotope effect on haloalkane dehalogenase activity. The activity (V_{obs}) was determined at increasing concentrations of ^2H_2O. The ratio between the dehalogenase activity in ^1H_2O (V_H) and in ^2H_2O (V_{obs}) was plotted vs various $^1H_2O/^2H_2O$ ratios: (■) 5 mM 1,3-dibromopropane, (▲) 2 mM 1,2,3-tribromopropane, (●) 10 mM 1,2,3-trichloropropane, and (□) 10 mM 1,2-dibromoethane as substrates.

Comparing the maximum turnover rates of DhaA with halopropanes using H_2O or ^2H_2O as a solvent provides information about the position of the slowest step in the catalytic cycle. A ^2H_2O solvent kinetic isotope effect on the maximum turnover rate is often indicative of the cleavage of H−X (X is N or O) bonds in the rate-determining step, but can also be due to a conformational change (*32*). Cleavage of an X−D bond is several times slower than that of an X−H bond. In the dehalogenase reaction, cleavage of an H−X bond occurs during hydrolysis of the alkyl−enzyme intermediate, a process that is facilitated by proton abstraction from water by the base catalyst histidine. However, experiments with DhlA showed that the catalytic rate was also decreased in ^2H_2O due to a decrease in the overall flexibility of a part of the protein that has to undergo a conformation change for allowing product release (*27*). Therefore, the use of deuterium oxide as a solvent is expected to reduce the maximum turnover rate if the slowest step is hydrolysis of the alkyl−enzyme intermediate or a slow step that requires conformational changes, but not if cleavage of the carbon−halogen bond is the slowest step.

The occurrence of a solvent kinetic isotope effect was tested for different halopropanes. In the presence of 95% deuterium oxide, V_H/V_{obs} ratios of 2.5 and 2 were found for 1,3-dibromopropane and 1,2,3-tribromopropane, respectively (Figure 1). With 1,2,3-trichloropropane, however, no such decrease in the k_{cat} was observed. Thus, during 1,2,3-trichloropropane conversion, there appears to be a different rate-determining step, i.e., carbon−chlorine bond cleavage (Figure 1). The kinetic mechanism of DhaA was further investigated by a transient kinetic approach using 1,3-dibromopropane as a model substrate because of the high affinity of the dehalogenase for this compound.

Transient-State Kinetic Analysis of 1,3-Dibromopropane Conversion. The chemical reaction steps involved in dehalogenation of 1,3-dibromopropane by DhaA were examined using rapid-quench-flow kinetic methods. To identify the rate-limiting step in the overall reaction pathway, we conducted a pre-steady-state burst experiment and followed product formation. The reaction was initiated by mixing an excess of 1,3-dibromopropane (final concentration of 2.5 mM) with DhaA (final concentration of 540 μM). After various times, the reactions were quenched and the amounts of bromide and 3-bromo-1-propanol were quantitated. A pre-steady-state burst was found both for bromide and 3-bromo-1-propanol, with observed exponential burst rate constants of 250 and 10 s^{-1}, respectively (Figure 2A). This fast initial rate was followed by a slower steady-state rate of product formation of 2.8 s^{-1} (k_{ss} divided by the active enzyme concentration), which is in good agreement with the k_{cat} of 2.7 s^{-1} determined from halide production rates that were found after manual mixing. The active enzyme concentration was obtained from the amplitude of the bromide burst and corresponded apparently to 65% of the enzyme concentration as was determined spectrophotometrically.

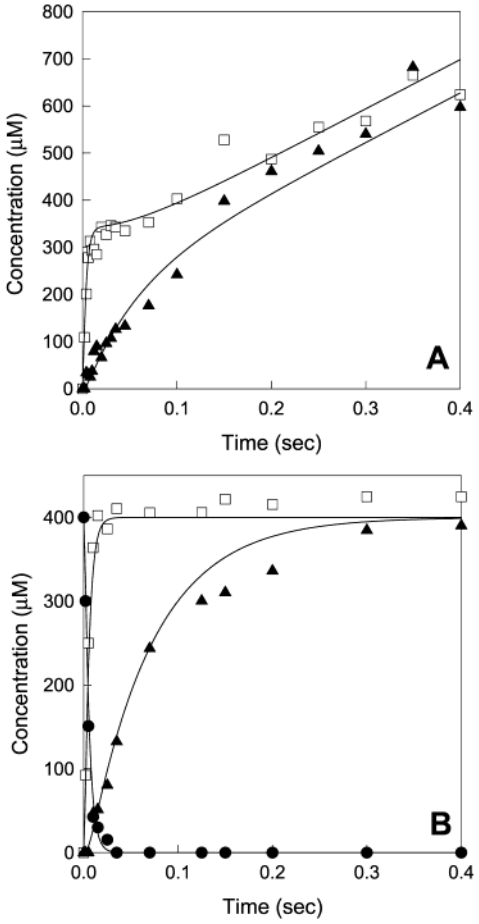

FIGURE 2: Dehalogenation of 1,3-dibromopropane under pre-steady-state conditions. (A) Pre-steady-state burst of bromide production (□) and 3-bromo-1-propanol production (▲). Reactions were conducted by mixing DhaA (520 μM) with excess 1,3-dibromopropane (2500 μM) in 50 mM $NaHCO_3$/NaOH (pH 9.4) and 1 mM dithiothreitol (pH 9.4). (B) Kinetics of a single turnover in 50 mM $NaHCO_3$/NaOH (pH 9.4). A solution of DhaA (750 μM) and 1,3-dibromopropane (400 μM) was mixed to initiate the reaction. The disappearance and formation of 1,3-dibromopropane (●), bromide (□), and 3-bromo-1-propanol (▲) were monitored. The curves are numerical fits generated with Dynafit using the rate constants summarized in Table 2.

The observation of a pre-steady-state burst for both products indicated that a step after chemical catalysis, presumably product release, is rate-limiting. Furthermore, it implies that there are at least three steps following substrate binding (Scheme 1): formation of the alkyl−enzyme intermediate (step 2), hydrolysis of the alkyl−enzyme intermedi-

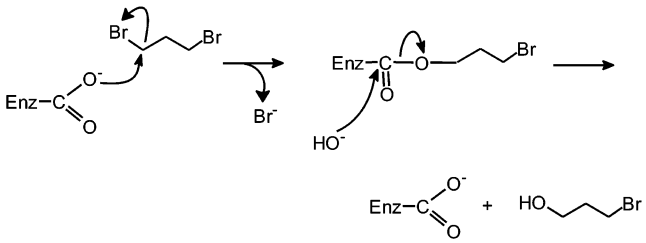

FIGURE 3: Reaction mechanism of haloalkane dehalogenase. After formation of the Michaelis complex, the dehalogenation reaction proceeds via a nucleophilic attack of an aspartate side chain on the halo-substituted carbon atom of the substrate, thereby displacing the halogen ion and forming an alkyl−enzyme intermediate. This covalent intermediate is subsequently hydrolyzed by a water molecule activated by the base catalyst histidine, yielding the (halo)-alcohol.

ate (step 3), and product release (step 4). Because the amount of bromide present during steady-state turnover was approximately the same as the amount of 3-bromo-1-propanol produced, there was no significant accumulation of a covalent enzyme−substrate intermediate, which is in agreement with a slow step occurring after hydrolysis of the intermediate. The exponential burst phases of bromide and 3-bromo-1-propanol production largely define rate constants k_2 and k_3, respectively. The steady-state rate k_{ss} defines the rate constant of product release k_4, which corresponds to a simplified step representing an unknown unimolecular rate-limiting event.

The kinetics of a single turnover of 1,3-dibromopropane conversion by DhaA are shown in Figure 2B. Excess DhaA (750 μM) was rapidly mixed with 1,3-dibromopropane (400 μM), and substrate depletion and product formation were monitored. Within the first 15 ms of the reaction, substrate disappeared and simultaneously bromide production reached its maximum, whereas hardly any 3-bromo-1-propanol was observed. Substrate depletion and 3-bromo-1-propanol production curves crossed at 70 μM, indicating that hydrolysis of the covalent intermediate occurred at a much lower rate than its formation. This resulted in a very rapid accumulation of the alkyl−enzyme intermediate. The initial dehalogenation step appears to be irreversible, since all halide was completely released during the initial phase of alcohol production.

Proposed Kinetic Mechanism for Haloalkane Dehalogenase DhaA. A minimal model consisting of four steps consistent with the pre-steady-state data (Figure 3 and Scheme 1) was constructed.

Scheme 1

$$E + RX \underset{k_{-1}}{\overset{k_1}{\rightleftharpoons}} E{\cdot}RX \xrightarrow{k_2} E{-}R{\cdot}X^- \xrightarrow{k_3} E{\cdot}ROH{\cdot}X^- \xrightarrow{k_4} E + ROH + X^-$$

The mechanism involves substrate binding, formation of an alkyl−enzyme intermediate and simultaneous cleavage of the carbon−bromine bond, hydrolysis of the alkyl−enzyme intermediate, and finally release of the products from the enzyme active site. On the basis of the observation of a product burst, the first three steps occur at a rate that is faster than the rate of steady-state turnover, whereas step 4, product release, is proposed to limit maximum turnover. The overall dehalogenase reaction was considered irreversible since no products are observed in the reverse reaction. To determine the rate constants for the individual steps, both pre-steady-state burst and single-turnover data were combined and fitted to the mechanism presented in Scheme 1 by numerical integration using Dynafit. The adjustable parameters were all five rate constants that appear in the reaction mechanism, and the resulting best fit values are summarized in Table 2. Initially, the amplitude of the bromide burst was lower than expected. A decreased burst amplitude may be governed by several factors, such as characteristics of the reaction kinetics, an internal equilibrium, or that a fraction of the enzyme is not participating in the reaction (*30*). In a recent paper, Lewandowicz et al. suggested, on the basis of the measurement of a chlorine kinetic isotope effect, that the dehalogenation step during conversion of 1,2-dichloroethane by DhlA is reversible and that the overall irreversibility is caused by the hydrolysis of the covalent intermediate (*33*). Therefore, we also performed burst simulations using a model that includes a reversible dehalogenation step. However, these simulations could not explain the data of both pre-steady-state burst and single-turnover experiments. Furthermore, the observation that during a single turnover essentially all substrate is transiently present as a covalent intermediate excludes reversibility of the first chemical step (see above). The mechanism presented in Scheme 1 could describe the experimental data if the active enzyme concentration present during the burst experiment was ~65% of the total amount of protein, indicating that a significant fraction of DhaA was not participating in the reaction under these conditions. Therefore, the concentration of DhaA was optimized for each data set. The best fit values of the optimized enzyme concentrations were 343 and 660 μM for the pre-steady-state burst and single-turnover experiment, respectively. The fits in panels A and B of Figure 2 were computed using the kinetic model of Scheme 1 and the rate constants in Table 2.

Table 2: Pre-Steady-State Kinetic Constants of DhaA for 1,3-Dibromopropane (Scheme 1) at pH 9.4 and 30 °C

reaction	kinetic parameter	value
substrate binding	k_1	1.0 μM^{-1} s^{-1} (0.8−2.5)
substrate dissociation[a]	k_{-1}	60−300 s^{-1}
carbon−bromine bond cleavage	k_2	300 s^{-1} (249−372)
hydrolysis of the alkyl−enzyme intermediate	k_3	14.8 s^{-1} (13.5−16.3)
product release	k_4	3.9 s^{-1} (3.4−4.6)

[a] Determined from steady-state parameters and computer simulation. Numbers in parentheses represent the 95% confidence intervals.

The results clearly show that substrate binding and chemical catalysis are not the steps that limit maximum turnover. Using single-turnover conditions, the rate of substrate binding appeared to be faster than the rate of chemical catalysis. At a 1,3-dibromopropane concentration of 400 μM, the pseudo-first-order rate constant (k_1[S]) was 400 s^{-1}. The data did not allow extraction of a unique value for the rate of substrate dissociation k_{-1}, but a solution could be obtained using computer simulations to the mechanism in Scheme 1 together with the rate constants in Table 2. These simulations were constrained by the experimental K_M and k_{cat}/K_M. The rate constants k_2−k_4 were determined by fitting the kinetic scheme to the rapid-quench data. Carbon−bromine bond cleavage and the simultaneous formation of the alkyl−enzyme intermediate (k_2) occurred with a rate of

300 s^{-1}. The rate of hydrolysis of the intermediate (k_3), obtained from the 3-bromo-1-propanol traces, was 20-fold lower but still higher than k_{cat}. The linear phase after the pre-steady-state burst defined the rate of product release (k_4) at 3.9 s^{-1}, and was close to the experimental k_{cat}. This step is simplified with a first-order rate constant, which could be a conformational change or another manner of slow release of products from the enzyme active site. Calculation of the steady-state kinetic parameters for a four-step kinetic model (Scheme 1), in which $k_{cat} = (k_2k_3k_4)/(k_2k_3 + k_2k_4 + k_3k_4)$, $K_M = [k_3k_4(k_{-1} + k_2)]/[k_1(k_2k_3 + k_2k_4 + k_3k_4)]$, and $k_{cat}/K_M = (k_1k_2)/(k_{-1} + k_2)$, using the obtained individual constants, yielded values which are in close agreement with the experimentally determined values, for both k_{cat} (3.0 s^{-1}) and K_M (3.7 μM).

A comparison of the mechanism of DhaA with that of DhlA showed a similar overall mechanism consisting of four main steps with a rate-limiting release of products from the active site. For DhlA, it was established using stopped-flow fluorescence quenching that the rate of release of the halide ion from the active site was limited by a conformational change in the cap domain that is necessary to allow water to enter the active site and solvate the halide ion (*27*). This conformational change separates the halide release step from the substrate binding step, which explains that halide is not a competitive inhibitor. Bromide also was not a competitive inhibitor in DhaA. Although release of the halide ion in DhaA cannot be assessed directly by stopped-flow fluorescence experiments, we have several reasons to propose that bromide release is probably not the rate-limiting step. In the first place, if for different brominated compounds bromide release would be rate-determining and the reaction sequence is the same, then they should all be hydrolyzed with the same value of k_{cat} (*20*). However, the high rate of hydrolysis of 1,2-dibromoethane by DhaA shows that bromide can be released at a rate of at least 14.3 s^{-1}, which is 4−5-fold faster than the maximum turnover rate with 1,3-dibromopropane. The rate-determining step for 1,2-dibromoethane conversion is also at the end of the reaction sequence as indicated by the occurrence of a ^2H_2O solvent kinetic isotope effect. In addition, product inhibition studies suggest that bromide exerts a noncompetitive type of inhibition on DhaA, and thus, bromide apparently does not interfere with substrate binding. Therefore, it is most likely that bromide is immediately released from the product-binding pocket after cleavage of the carbon−bromine bond. Hence, it seems plausible that the release of the product alcohol from the active site is rate-determining. The difference in k_{cat} between 1,2-dibromoethane and 1,3-dibromopropane might then be due to a faster diffusion of 2-bromoethanol out of the active site than of 3-bromo-1-propanol. DhaA also has a higher affinity for the latter halohydrin. Nevertheless, a different rate-determining step for 1,2-dibromoethane could not be excluded.

Another reason to assume that bromide is not the last product released from the active site comes from examination of the crystal structures of DhaA and DhlA. With both dehalogenases, the active site cavity is lined with mainly hydrophobic residues providing an optimal microenvironment, with respect to charge and polarity and by stabilizing reaction intermediates, for the efficient conversion of substrate to product. Export of the halide ion from the active site cavity into the solvent requires ion destabilization and solvation of the halide ion by water. Compared to DhlA, the active site of DhaA is connected to the solvent by a much larger tunnel and is less buried in the protein core (*12*). In addition, Newman et al. suggested that at pH 7−9, where the enzyme activity is measured, the cap domain of DhaA becomes more flexible (*13*). These observations suggest that the accessibility of water to the active site may be facilitated, allowing a faster exchange of the halide ions and water with the bulk solvent. Furthermore, while DhaA and DhlA are considerably homologous in sequence and structure in the central catalytic domain, there are some differences in the active site residues involved in catalysis which might influence different kinetic steps (*21*). In DhlA, Trp125 forms a halide-binding site in the active site together with Trp175. The function of the latter tryptophan residue is probably fulfilled by a Phe and Asn residue in DhaA, which is proposed to result in weaker binding of the halide ion that is cleaved off (*12*, *21*). Another structural feature that may facilitate halide release in DhaA is the different topological position of the carboxylate functionality of the triad. The triad acid group in DhaA follows β-strand 6 rather than β-strand 7 as in DhlA and most other α/β-hydrolase fold enzymes (*13*, *22*). Mutagenesis of active site residues Trp175 and Asp260 of DhlA, and subsequent structural and kinetic analysis, corroborated the above observations. These experiments showed that halide release in these mutants was accelerated and not limiting maximum turnover as was found for wild-type DhlA (*34*, *35*).

Summarizing, we defined the steps of a minimal dehalogenation mechanism that is sufficient to explain the steady-state kinetic data. Pre-steady-state kinetic analysis of 1,3-dibromopropane conversion by DhaA showed that substrate binding and chemical catalysis occur faster than the steady-state rate which corresponds to product release. The overall mechanism by which DhaA catalyzes dehalogenation is similar to that of DhlA, but the rate-determining step of DhaA may be different. In DhaA, the less efficient stabilization of the leaving halogen, the different topological arrangement of the triad acid Glu130, and the much larger and less buried active site cavity may allow faster diffusion of the halide ion out of the active site. Together with the high activity on 1,2-dibromoethane, these observations support the idea that bromide release is not rate-determining during conversion of 1,3-dibromopropane. Release of the product alcohol from the DhaA active site is therefore proposed to be the overall rate-limiting step, which is largely determined by the size and affinity of the product alcohol, explaining the difference in k_{cat} between 1,2-dibromoethane and 1,3-dibromopropane conversion.

REFERENCES

1. van Agteren, M. H., Keuning, S., and Janssen, D. B. (1998) *Biodegradation and Biological Treatment of Hazardous Organic Compounds*, Kluwer Academic Publishers, Dordrecht, The Netherlands.
2. Swanson, P. E. (1999) *Curr. Opin. Biotechnol. 10*, 365−369.
3. Keuning, S., Janssen, D. B., and Witholt, B. (1985) *J. Bacteriol. 163*, 635−639.
4. Nagata, Y., Miyauchi, K., Damborsky, J., Manova, K., Ansorgova, A., and Takagi, M. (1997) *Appl. Environ. Microbiol. 63*, 3707−3710.
5. Kulakova, A. N., Larkin, M. J., and Kulakov, L. A. (1997) *Microbiology 143*, 109−115.
6. Yokota, T., Omori, T., and Kodama, T. (1987) *J. Bacteriol. 169*, 4049−4054.

7. Scholtz, R., Leisinger, T., Suter, F., and Cook, A. M. (1987) *J. Bacteriol. 169*, 5016−5021.
8. Janssen, D. B., Gerritse, J., Brackman, J., Kalk, C., Jager, D., and Witholt, B. (1988) *Eur. J. Biochem. 171*, 67−72.
9. Sallis, P. J., Armfield, S. J., Bull, A. T., and Hardman, D. J. (1990) *J. Gen. Microbiol. 136*, 115−120.
10. Poelarends, G. J., Zandstra, M., Bosma, T., Kulakov, L. A., Larkin, M. J., Marchesi, J. R., Weightman, A. J., and Janssen, D. B. (2000) *J. Bacteriol. 182*, 2725−2731.
11. Verschueren, K. H., Franken, S. M., Rozeboom, H. J., Kalk, K. H., and Dijkstra, B. W. (1993) *J. Mol. Biol. 232*, 856−872.
12. Marek, J., Vevodova, J., Smatanova, I. K., Nagata, Y., Svensson, L. A., Newman, J., Takagi, M., and Damborsky, J. (2000) *Biochemistry 39*, 14082−14086.
13. Newman, J., Peat, T. S., Richard, R., Kan, L., Swanson, P. E., Affholter, J. A., Holmes, I. H., Schindler, J. F., Unkefer, T. C., and Terwilliger, T. C. (1999) *Biochemistry 38*, 16105−16114.
14. Ollis, D. L., Cheah, E., Cygler, M., Dijkstra, B., Frolow, N., Franken, S. M., Harel, M., Remington, S. J., Silman, I., Schrag, J., Sussman, J. L., Verschueren, K. H. G., and Goldman, A. (1992) *Protein Eng. 5*, 197−211.
15. Pries, F., Wijngaard, A. J., Bos, R., Pentenga, M., and Janssen, D. B. (1994) *J. Biol. Chem. 269*, 17490−17494.
16. Verschueren, K. H. G., Seljee, F., Rozeboom, H. J., Kalk, K. H., and Dijkstra, B. W. (1993) *Nature 363*, 693−698.
17. Pries, F., Kingma, J., Pentenga, M., Van Pouderoyen, G., Jeronimus-Stratingh, C. M., Bruins, A. P., and Janssen, D. B. (1994) *Biochemistry 33*, 1242−1247.
18. Pries, F., Kingma, J., Krooshof, G. H., Jeronimus-Stratingh, C. M., Bruins, A. P., and Janssen, D. B. (1995) *J. Biol. Chem. 270*, 10405−10411.
19. Pries, F., Kingma, J., and Janssen, D. B. (1995) *FEBS Lett. 358*, 171−174.
20. Schanstra, J. P., Kingma, J., and Janssen, D. B. (1996) *J. Biol. Chem. 271*, 14747−14753.
21. Damborsky, J., and Koca, J. (1999) *Protein Eng. 12*, 989−998.
22. Heikinheimo, P., Goldman, A., Jeffries, C., and Ollis, D. L. (1999) *Structure 7*, R141−R146.
23. Gray, K. A., Richardson, T. H., Kretz, K., Short, J. M., Bartnek, F., Knowles, R., Kan, L., Swanson, P. E., and Robertson, D. E. (2001) *Adv. Synth. Catal. 343*, 607−617.
24. Bosma, T., Damborsky, J., Stucki, G., and Janssen, D. B. (2002) *Appl. Environ. Microbiol. 68*, 3582−3587.
25. Schindler, J. F., Naranjo, P. A., Honaberger, D. A., Chang, C.-H., Brainard, J. R., Vanderberg, L. A., and Unkefer, C. J. (1999) *Biochemistry 38*, 5772−5778.
26. Bosma, T., Kruizinga, E., de Bruin, E. J., Poelarends, G. J., and Janssen, D. B. (1999) *Appl. Environ. Microbiol. 65*, 4575−4581.
27. Schanstra, J. P., and Janssen, D. B. (1996) *Biochemistry 35*, 5624−5632.
28. Schanstra, J. P., Rink, R., Pries, F., and Janssen, D. B. (1993) *Protein Expression Purif. 4*, 479−489.
29. Kuzmic, P. (1996) *Anal. Biochem. 237*, 260−273.
30. Johnson, K. (1992) *Enzymes 20*, 1−61.
31. Verschueren, K. H., Kingma, J., Rozeboom, H. J., Kalk, K. H., Janssen, D. B., and Dijkstra, B. W. (1993) *Biochemistry 32*, 9031−9037.
32. Tuena de Gómez-Puyou, M., Gómez-Puyou, A., and Cerbon, J. (1978) *Arch. Biochem. Biophys. 187*, 72−77.
33. Lewandowicz, A., Rudzinski, J., Tronstad, L., Widersten, M., Ryberg, P., Matsson, O., and Paneth, P. (2001) *J. Am. Chem. Soc. 123*, 4550−4555.
34. Kennes, C., Pries, F., Krooshof, G. H., Bokma, E., Kingma, J., and Janssen, D. B. (1995) *Eur. J. Biochem. 228*, 403−407.
35. Krooshof, G. H., Kwant, E. M., Damborsky, J., Koca, J., and Janssen, D. B. (1997) *Biochemistry 36*, 9571−9580.

BI026907M